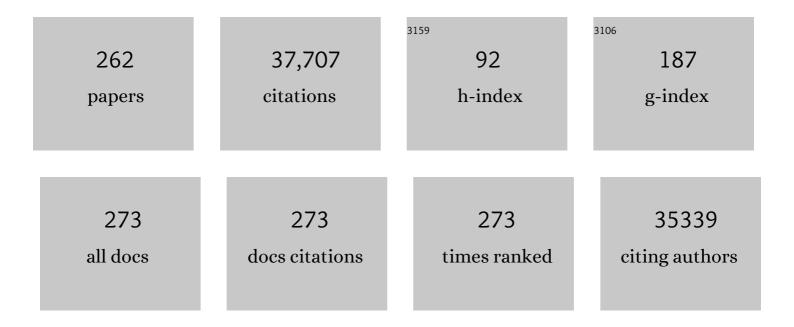
## List of Publications by Year in descending order

Source: https://exaly.com/author-pdf/4638604/publications.pdf

Version: 2024-02-01



RINLIII

#	Article	IF	CITATIONS
1	Amorphous alloys for electrocatalysis: The significant role of the amorphous alloy structure. Nano Research, 2023, 16, 4277-4288.	10.4	32
2	Atomically-dispersed NiN <sub>4</sub> –Cl active sites with axial Ni–Cl coordination for accelerating electrocatalytic hydrogen evolution. Journal of Materials Chemistry A, 2022, 10, 6007-6015.	10.3	22
3	Strong Metal–Support Interaction Boosts Activity, Selectivity, and Stability in Electrosynthesis of H <sub>2</sub> O <sub>2</sub> . Journal of the American Chemical Society, 2022, 144, 2255-2263.	13.7	90
4	Hierarchical trace copper incorporation activated cobalt layered double hydroxide as a highly selective methanol conversion electrocatalyst to realize energy-matched photovoltaic-electrocatalytic formate and hydrogen co-production. Journal of Materials Chemistry A, 2022, 10, 19649-19661.	10.3	12
5	Boosting ORR performance by single atomic divacancy Zn–N3C–C8 sites on ultrathin N-doped carbon nanosheets. Chem Catalysis, 2022, 2, 836-852.	6.1	25
6	Constructing partially amorphous borate doped iron-nickel nitrate hydroxide nanoarrays by rapid microwave activation for oxygen evolution. Applied Surface Science, 2022, 592, 153245.	6.1	6
7	Efficient and Selective CO <sub>2</sub> Reduction to Formate on Pdâ€Doped Pb <sub>3</sub> (CO <sub>3</sub> ) <sub>2</sub> (OH) <sub>2</sub> : Dynamic Catalyst Reconstruction and Accelerated CO <sub>2</sub> Protonation. Small, 2022, 18, e2107885.	10.0	18
8	Understanding the Effect of *CO Coverage on C–C Coupling toward CO <sub>2</sub> Electroreduction. Nano Letters, 2022, 22, 3801-3808.	9.1	44
9	Enhancing the Mechanical Robustness of Gold Nanowire Array via Sulfideâ€Mediated Growth. Small Structures, 2022, 3, .	12.0	3
10	Polarization Engineering of Covalent Triazine Frameworks for Highly Efficient Photosynthesis of Hydrogen Peroxide from Molecular Oxygen and Water. Advanced Materials, 2022, 34, e2110266.	21.0	136
11	Ruthenium/titanium oxide interface promoted electrochemical nitrogen reduction reaction. Chem Catalysis, 2022, 2, 1764-1774.	6.1	6
12	Recent Advances in Carbonâ€5upported Nobleâ€Metal Electrocatalysts for Hydrogen Evolution Reaction: Syntheses, Structures, and Properties. Advanced Energy Materials, 2022, 12, .	19.5	64
13	Identifying Activity Trends for the Electrochemical Production of H <sub>2</sub> O <sub>2</sub> on M–N–C Single-Atom Catalysts Using Theoretical Kinetic Computations. Journal of Physical Chemistry C, 2022, 126, 10388-10398.	3.1	12
14	Rational design of donor-acceptor conjugated polymers with high performance on peroxydisulfate activation for pollutants degradation. Applied Catalysis B: Environmental, 2022, 316, 121611.	20.2	73
15	Unraveling the Mechanism on Ultrahigh Efficiency Photocatalytic H <sub>2</sub> O <sub>2</sub> Generation for Dualâ€Heteroatom Incorporated Polymeric Carbon Nitride. Advanced Functional Materials, 2022, 32, .	14.9	100
16	Kinetic Insights of Proton Exchange Membrane Water Electrolyzer Obtained by <i>Operando</i> Characterization Methods. Journal of Physical Chemistry Letters, 2022, 13, 6520-6531.	4.6	12
17	Van der Waals heterojunction for selective visible-light-driven photocatalytic CO2 reduction. Applied Catalysis B: Environmental, 2021, 284, 119733.	20.2	92
18	Coordination Engineering of Singleâ€Atom Catalysts for the Oxygen Reduction Reaction: A Review. Advanced Energy Materials, 2021, 11, 2002473.	19.5	217

#	Article	IF	CITATIONS
19	Noble metal nanowire arrays as an ethanol oxidation electrocatalyst. Nanoscale Advances, 2021, 3, 177-181.	4.6	6
20	Real-time photoelectrochemical quantification of hydrogen peroxide produced by living cells. Chemical Engineering Journal, 2021, 407, 127203.	12.7	32
21	How does mass transfer influence electrochemical carbon dioxide reduction reaction? A case study of Ni molecular catalyst supported on carbon. Chemical Communications, 2021, 57, 1384-1387.	4.1	18
22	Halide perovskite composites for photocatalysis: A mini review. EcoMat, 2021, 3, e12079.	11.9	60
23	Atomically Dispersed Fe–Heteroatom (N, S) Bridge Sites Anchored on Carbon Nanosheets for Promoting Oxygen Reduction Reaction. ACS Energy Letters, 2021, 6, 379-386.	17.4	167
24	Ordered clustering of single atomic Te vacancies in atomically thin PtTe2 promotes hydrogen evolution catalysis. Nature Communications, 2021, 12, 2351.	12.8	83
25	Atomically dispersed antimony on carbon nitride for the artificial photosynthesis of hydrogen peroxide. Nature Catalysis, 2021, 4, 374-384.	34.4	474
26	In-Situ doping-induced crystal form transition of amorphous Pd–P catalyst for robust electrocatalytic hydrodechlorination. Applied Catalysis B: Environmental, 2021, 284, 119713.	20.2	41
27	Unveiling the In Situ Generation of a Monovalent Fe(I) Site in the Single-Fe-Atom Catalyst for Electrochemical CO <sub>2</sub> Reduction. ACS Catalysis, 2021, 11, 7292-7301.	11.2	51
28	Phosphorus modified carbon fiber cloth as a robust and efficient anode for alkaline water electrolysis. Materials Today Energy, 2021, 20, 100683.	4.7	2
29	Progress of Nonpreciousâ€Metalâ€Based Electrocatalysts for Oxygen Evolution in Acidic Media. Advanced Materials, 2021, 33, e2003786.	21.0	166
30	Orbital coupling of hetero-diatomic nickel-iron site for bifunctional electrocatalysis of CO2 reduction and oxygen evolution. Nature Communications, 2021, 12, 4088.	12.8	259
31	Atomically dispersed Pd electrocatalyst for efficient aqueous phase dechlorination reaction. Electrochimica Acta, 2021, 391, 138886.	5.2	20
32	In situ/operando Mössbauer spectroscopy for probing heterogeneous catalysis. Chem Catalysis, 2021, 1, 1215-1233.	6.1	24
33	Boosting Hydrogen Evolution Reaction via Electronic Coupling of Cerium Phosphate with Molybdenum Phosphide Nanobelts. Small, 2021, 17, e2102413.	10.0	27
34	Dynamic Restructuring of Cuâ€Đoped SnS <sub>2</sub> Nanoflowers for Highly Selective Electrochemical CO <sub>2</sub> Reduction to Formate. Angewandte Chemie, 2021, 133, 26437-26441.	2.0	8
35	<i>In Situ</i> Precise Tuning of Bimetallic Electronic Effect for Boosting Oxygen Reduction Catalysis. Nano Letters, 2021, 21, 7753-7760.	9.1	24
36	Dynamic Restructuring of Cuâ€Đoped SnS <sub>2</sub> Nanoflowers for Highly Selective Electrochemical CO <sub>2</sub> Reduction to Formate. Angewandte Chemie - International Edition, 2021, 60, 26233-26237.	13.8	66

#	Article	IF	CITATIONS
37	Ni <sub>2</sub> P Interlayer and Mn Doping Synergistically Expedite the Hydrogen Evolution Reaction Kinetics of Co <sub>2</sub> P. Chemistry - A European Journal, 2021, 27, 3536-3541.	3.3	10
38	Ultrafine Co <sub>6</sub> W <sub>6</sub> C as an efficient anode catalyst for direct hydrazine fuel cells. Chemical Communications, 2021, 57, 10415-10418.	4.1	6
39	Recent advances in single atom catalysts for the electrochemical carbon dioxide reduction reaction. Chemical Science, 2021, 12, 6800-6819.	7.4	130
40	Microwave hydrothermally synthesized WO3/UiO-66 nanocomposites toward enhanced photocatalytic degradation of rhodamine B. Advanced Composites and Hybrid Materials, 2021, 4, 1330-1342.	21.1	57
41	Boosting Hydrogen Evolution Reaction via Electronic Coupling of Cerium Phosphate with Molybdenum Phosphide Nanobelts (Small 40/2021). Small, 2021, 17, 2170208.	10.0	5
42	Electrochemical Reduction of CO <sub>2</sub> to CO over Transition Metal/Nâ€Doped Carbon Catalysts: The Active Sites and Reaction Mechanism. Advanced Science, 2021, 8, e2102886.	11.2	121
43	Electrochemical looping hydrogen production at room temperature. Chem Catalysis, 2021, 1, 1365-1366.	6.1	1
44	Elucidating the Electrocatalytic CO <sub>2</sub> Reduction Reaction over a Model Singleâ€Atom Nickel Catalyst. Angewandte Chemie - International Edition, 2020, 59, 798-803.	13.8	315
45	Elucidating the Electrocatalytic CO <sub>2</sub> Reduction Reaction over a Model Singleâ€Atom Nickel Catalyst. Angewandte Chemie, 2020, 132, 808-813.	2.0	33
46	Polyvinyl Chlorideâ€Derived Carbon Spheres for CO <sub>2</sub> Adsorption. ChemSusChem, 2020, 13, 6426-6432.	6.8	31
47	Amorphous/Crystalline Heterostructured Cobaltâ€Vanadiumâ€Iron (Oxy)hydroxides for Highly Efficient Oxygen Evolution Reaction. Advanced Energy Materials, 2020, 10, 2002215.	19.5	198
48	Identification of the Electronic and Structural Dynamics of Catalytic Centers in Single-Fe-Atom Material. CheM, 2020, 6, 3440-3454.	11.7	231
49	Boosting oxygen evolution reaction on graphene through engineering electronic structure. Carbon, 2020, 170, 414-420.	10.3	26
50	Adaptive Bifunctional Electrocatalyst of Amorphous CoFe Oxide @ 2D Black Phosphorus for Overall Water Splitting. Angewandte Chemie, 2020, 132, 21292-21299.	2.0	26
51	Adaptive Bifunctional Electrocatalyst of Amorphous CoFe Oxide @ 2D Black Phosphorus for Overall Water Splitting. Angewandte Chemie - International Edition, 2020, 59, 21106-21113.	13.8	182
52	Hybridization of Bimetallic Molybdenumâ€Tungsten Carbide with Nitrogenâ€Doped Carbon: A Rational Design of Super Active Porous Composite Nanowires with Tailored Electronic Structure for Boosting Hydrogen Evolution Catalysis. Advanced Functional Materials, 2020, 30, 2003198.	14.9	57
53	Atomically-precise dopant-controlled single cluster catalysis for electrochemical nitrogen reduction. Nature Communications, 2020, 11, 4389.	12.8	110
54	Microenvironment modulation of single-atom catalysts and their roles in electrochemical energy conversion. Science Advances, 2020, 6, .	10.3	214

#	Article	IF	CITATIONS
55	Coordination engineering of iridium nanocluster bifunctional electrocatalyst for highly efficient and pH-universal overall water splitting. Nature Communications, 2020, 11, 4246.	12.8	221
56	Tuning the Electronic Structures of Multimetal Oxide Nanoplates to Realize Favorable Adsorption Energies of Oxygenated Intermediates. ACS Nano, 2020, 14, 17640-17651.	14.6	56
57	Electron-withdrawing functional ligand promotes CO2 reduction catalysis in single atom catalyst. Science China Chemistry, 2020, 63, 1727-1733.	8.2	49
58	Dual single-site catalyst promoter boosts catalytic performance. National Science Review, 2020, 7, 1841-1842.	9.5	4
59	Amorphous Multimetal Alloy Oxygen Evolving Catalysts. , 2020, 2, 624-632.		45
60	Rational Design of an Iridium–Tungsten Composite with an Iridium-Rich Surface for Acidic Water Oxidation. ACS Applied Materials & Interfaces, 2020, 12, 25991-26001.	8.0	36
61	Amorphous versus Crystalline in Water Oxidation Catalysis: A Case Study of NiFe Alloy. Nano Letters, 2020, 20, 4278-4285.	9.1	201
62	Metal organic frameworks for adsorption-based separation of fluorocompounds: a review. Materials Advances, 2020, 1, 310-320.	5.4	53
63	High performance Ni catalysts prepared by freeze drying for efficient dry reforming of methane. Applied Catalysis B: Environmental, 2020, 275, 119109.	20.2	60
64	Single-Ni-atom catalyzes aqueous phase electrochemical reductive dechlorination reaction. Applied Catalysis B: Environmental, 2020, 277, 119057.	20.2	51
65	Advances in Thermodynamic-Kinetic Model for Analyzing the Oxygen Evolution Reaction. ACS Catalysis, 2020, 10, 8597-8610.	11.2	89
66	Tuning reactivity of Fischer–Tropsch synthesis by regulating TiOx overlayer over Ru/TiO2 nanocatalysts. Nature Communications, 2020, 11, 3185.	12.8	114
67	Progress of Electrochemical Hydrogen Peroxide Synthesis over Single Atom Catalysts. , 2020, 2, 1008-1024.		129
68	Carbonâ€based cathode materials for rechargeable zincâ€eir batteries: From current collectors to bifunctional integrated air electrodes. , 2020, 2, 370-386.		82
69	Design of hierarchical, threeâ€dimensional freeâ€standing singleâ€atom electrode for H <sub>2</sub> O <sub>2</sub> production in acidic media. , 2020, 2, 276-282.		56
70	A general method to construct single-atom catalysts supported on N-doped graphene for energy applications. Journal of Materials Chemistry A, 2020, 8, 6190-6195.	10.3	41
71	The nonmetal modulation of composition and morphology of g-C3N4-based photocatalysts. Applied Catalysis B: Environmental, 2020, 269, 118828.	20.2	237
72	In-situ phase transition of WO3 boosting electron and hydrogen transfer for enhancing hydrogen evolution on Pt. Nano Energy, 2020, 71, 104653.	16.0	149

#	Article	IF	CITATIONS
73	Enabling Direct H2O2 Production in Acidic Media through Rational Design of Transition Metal Single Atom Catalyst. CheM, 2020, 6, 658-674.	11.7	418
74	Plasmon-enhanced photoelectrochemical water splitting by InGaN/GaN nano-photoanodes. Semiconductor Science and Technology, 2020, 35, 025017.	2.0	17
75	Electrostatic self-assembly of a AgI/Bi <sub>2</sub> Ga <sub>4</sub> O <sub>9</sub> p–n junction photocatalyst for boosting superoxide radical generation. Journal of Materials Chemistry A, 2020, 8, 4083-4090.	10.3	73
76	Pre-deposited Co nanofilms promoting high alloying degree of Pd Au nanoparticles as electrocatalysts in alkaline media. International Journal of Hydrogen Energy, 2020, 45, 28024-28033.	7.1	4
77	Atomically Dispersed Nickel(I) on an Alloyâ€Encapsulated Nitrogenâ€Doped Carbon Nanotube Array for Highâ€Performance Electrochemical CO <sub>2</sub> Reduction Reaction. Angewandte Chemie, 2020, 132, 12153-12159.	2.0	27
78	Atomically Dispersed Nickel(I) on an Alloyâ€Encapsulated Nitrogenâ€Doped Carbon Nanotube Array for Highâ€Performance Electrochemical CO <sub>2</sub> Reduction Reaction. Angewandte Chemie - International Edition, 2020, 59, 12055-12061.	13.8	117
79	Making fully printed perovskite solar cells stable outdoor with inorganic superhydrophobic coating. Journal of Energy Chemistry, 2020, 50, 332-338.	12.9	18
80	Self-assembly of three-dimensional CdS nanosphere/graphene networks for efficient photocatalytic hydrogen evolution. Journal of Energy Chemistry, 2019, 31, 34-38.	12.9	35
81	Revealing Energetics of Surface Oxygen Redox from Kinetic Fingerprint in Oxygen Electrocatalysis. Journal of the American Chemical Society, 2019, 141, 13803-13811.	13.7	151
82	Rational design of carbon-based metal-free catalysts for electrochemical carbon dioxide reduction: A review. Journal of Energy Chemistry, 2019, 36, 95-105.	12.9	91
83	Nanowire Photoelectrochemistry. Chemical Reviews, 2019, 119, 9221-9259.	47.7	158
84	Supported Nobleâ€Metal Single Atoms for Heterogeneous Catalysis. Advanced Materials, 2019, 31, e1902031.	21.0	207
85	Catalyst: Single-Atom Catalysis: Directing the Way toward the Nature of Catalysis. CheM, 2019, 5, 2733-2735.	11.7	57
86	Layered Structure Causes Bulk NiFe Layered Double Hydroxide Unstable in Alkaline Oxygen Evolution Reaction. Advanced Materials, 2019, 31, e1903909.	21.0	345
87	Bifunctional N-CoSe <sub>2</sub> /3D-MXene as Highly Efficient and Durable Cathode for Rechargeable Zn–Air Battery. , 2019, 1, 432-439.		90
88	Photoelectrochemical CO <sub>2</sub> reduction to adjustable syngas on grain-boundary-mediated a-Si/TiO <sub>2</sub> /Au photocathodes with low onset potentials. Energy and Environmental Science, 2019, 12, 923-928.	30.8	114
89	Breaking Long-Range Order in Iridium Oxide by Alkali Ion for Efficient Water Oxidation. Journal of the American Chemical Society, 2019, 141, 3014-3023.	13.7	337
90	Nanostructuring Confinement for Controllable Interfacial Charge Transfer. Small, 2019, 15, e1804391.	10.0	13

#	Article	IF	CITATIONS
91	A General Method to Probe Oxygen Evolution Intermediates at Operating Conditions. Joule, 2019, 3, 1498-1509.	24.0	243
92	Selective photoelectrochemical oxidation of glycerol to high value-added dihydroxyacetone. Nature Communications, 2019, 10, 1779.	12.8	185
93	Breaking the symmetry: Gradient in NiFe layered double hydroxide nanoarrays for efficient oxygen evolution. Nano Energy, 2019, 60, 661-666.	16.0	52
94	In Situ/Operando Techniques for Characterization of Single-Atom Catalysts. ACS Catalysis, 2019, 9, 2521-2531.	11.2	296
95	Expedient synthesis of <i>E</i> -hydrazone esters and 1 <i>H</i> -indazole scaffolds through heterogeneous single-atom platinum catalysis. Science Advances, 2019, 5, eaay1537.	10.3	31
96	NiFe Hydroxide Lattice Tensile Strain: Enhancement of Adsorption of Oxygenated Intermediates for Efficient Water Oxidation Catalysis. Angewandte Chemie, 2019, 131, 746-750.	2.0	55
97	The Absence and Importance of Operando Techniques for Metalâ€Free Catalysts. Advanced Materials, 2019, 31, e1805609.	21.0	25
98	Preparation of Ni(OH)2/TiO2 porous film with novel structure and electrochromic property. Solar Energy Materials and Solar Cells, 2019, 191, 108-116.	6.2	24
99	NiFe Hydroxide Lattice Tensile Strain: Enhancement of Adsorption of Oxygenated Intermediates for Efficient Water Oxidation Catalysis. Angewandte Chemie - International Edition, 2019, 58, 736-740.	13.8	335
100	Phase interactions in Ni-Cu-Al2O3 mixed oxide oxygen carriers for chemical looping applications. Applied Energy, 2019, 236, 635-647.	10.1	33
101	Organic-inorganic hybrid perovskite – TiO2 nanorod arrays for efficient and stable photoelectrochemical hydrogen evolution from HI splitting. Materials Today Chemistry, 2019, 12, 1-6.	3.5	32
102	Single-Atom Catalysis toward Efficient CO <sub>2</sub> Conversion to CO and Formate Products. Accounts of Chemical Research, 2019, 52, 656-664.	15.6	348
103	N, P dual-doped hollow carbon spheres supported MoS2 hybrid electrocatalyst for enhanced hydrogen evolution reaction. Catalysis Today, 2019, 330, 259-267.	4.4	39
104	Holey nickel hydroxide nanosheets for wearable solid-state fiber-supercapacitors. Nanoscale, 2018, 10, 5442-5448.	5.6	50
105	Assembly and photochemical properties of mesoporous networks of spinel ferrite nanoparticles for environmental photocatalytic remediation. Applied Catalysis B: Environmental, 2018, 227, 330-339.	20.2	51
106	Anchoring Mn <sub>3</sub> O <sub>4</sub> Nanoparticles on Oxygen Functionalized Carbon Nanotubes as Bifunctional Catalyst for Rechargeable Zinc-Air Battery. ACS Applied Energy Materials, 2018, 1, 963-969.	5.1	80
107	Fluorocarbon Separation in a Thermally Robust Zirconium Carboxylate Metal–Organic Framework. Chemistry - an Asian Journal, 2018, 13, 977-981.	3.3	16
108	Identifying Active Sites of Nitrogenâ€Doped Carbon Materials for the CO <sub>2</sub> Reduction Reaction. Advanced Functional Materials, 2018, 28, 1800499.	14.9	244

#	Article	IF	CITATIONS
109	In Situ/Operando Characterization Techniques to Probe the Electrochemical Reactions for Energy Conversion. Small Methods, 2018, 2, 1700395.	8.6	131
110	An Earthâ€Abundant Catalystâ€Based Seawater Photoelectrolysis System with 17.9% Solarâ€ŧoâ€Hydrogen Efficiency. Advanced Materials, 2018, 30, e1707261.	21.0	189
111	Tuning the Electronic Spin State of Catalysts by Strain Control for Highly Efficient Water Electrolysis. Small Methods, 2018, 2, 1800001.	8.6	70
112	Atomically dispersed Ni(i) as the active site for electrochemical CO2 reduction. Nature Energy, 2018, 3, 140-147.	39.5	1,594
113	Ultrasmall Transition Metal Carbide Nanoparticles Encapsulated in N, Sâ€Doped Graphene for Allâ€pH Hydrogen Evolution. Small Methods, 2018, 2, 1700353.	8.6	53
114	High-Performance Ni–Fe Redox Catalysts for Selective CH <sub>4</sub> to Syngas Conversion via Chemical Looping. ACS Catalysis, 2018, 8, 1748-1756.	11.2	72
115	Plasmonâ€Dictated Photoâ€Electrochemical Water Splitting for Solarâ€ŧoâ€Chemical Energy Conversion: Current Status and Future Perspectives. Advanced Materials Interfaces, 2018, 5, 1701098.	3.7	92
116	High Spin State Promotes Water Oxidation Catalysis at Neutral pH in Spinel Cobalt Oxide. Industrial & Engineering Chemistry Research, 2018, 57, 1441-1445.	3.7	28
117	Surface Rutilization of Anatase TiO2 for Efficient Electron Extraction and Stable Pmax Output of Perovskite Solar Cells. CheM, 2018, 4, 911-923.	11.7	28
118	Hydrogenated TiO2 nanosheet based flowerlike architectures: Enhanced sensing performances and sensing mechanism. Journal of Alloys and Compounds, 2018, 749, 543-555.	5.5	14
119	Fabrication of 3D mesoporous networks of assembled CoO nanoparticles for efficient photocatalytic reduction of aqueous Cr(VI). Applied Catalysis B: Environmental, 2018, 221, 635-644.	20.2	85
120	Unique role of Mössbauer spectroscopy in assessing structural features of heterogeneous catalysts. Applied Catalysis B: Environmental, 2018, 224, 518-532.	20.2	83
121	Homologous Co <sub>3</sub> O <sub>4</sub> ‖CoP nanowires grown on carbon cloth as a high-performance electrode pair for triclosan degradation and hydrogen evolution. Materials Chemistry Frontiers, 2018, 2, 323-330.	5.9	37
122	Boosting oxygen reaction activity by coupling sulfides for high-performance rechargeable metal–air battery. Journal of Materials Chemistry A, 2018, 6, 21162-21166.	10.3	38
123	Nitrogen and sulfur Co-doped graphene inlaid with cobalt clusters for efficient oxygen reduction reaction. Materials Today Energy, 2018, 10, 184-190.	4.7	24
124	Shape-Controlled Synthesis of Metal–Organic Frameworks with Adjustable Fenton-Like Catalytic Activity. ACS Applied Materials & Interfaces, 2018, 10, 38051-38056.	8.0	48
125	Aqueous-phase hydrodechlorination of 4-chlorophenol on palladium nanocrystals: Identifying the catalytic sites and unraveling the reaction mechanism. Journal of Catalysis, 2018, 368, 336-344.	6.2	38
126	Single Cobalt Atoms Anchored on Porous N-Doped Graphene with Dual Reaction Sites for Efficient Fenton-like Catalysis. Journal of the American Chemical Society, 2018, 140, 12469-12475.	13.7	1,044

#	Article	IF	CITATIONS
127	Molecular modulation of fluorene-dibenzothiophene- <i>S</i> , <i>S</i> -dioxide-based conjugated polymers for enhanced photoelectrochemical water oxidation under visible light. Materials Chemistry Frontiers, 2018, 2, 2021-2025.	5.9	12
128	Novel design of photoelectrochemical device by dual BiVO4 photoelectrode with abundant oxygen vacancy. Science Bulletin, 2018, 63, 1027-1028.	9.0	4
129	Mesoporous implantable Pt/SrTiO3:C,N nanocuboids delivering enhanced photocatalytic H2-production activity via plasmon-induced interfacial electron transfer. Applied Catalysis B: Environmental, 2018, 236, 338-347.	20.2	35
130	Iron Vacancies Induced Bifunctionality in Ultrathin Feroxyhyte Nanosheets for Overall Water Splitting. Advanced Materials, 2018, 30, e1803144.	21.0	225
131	<i>In situ</i> growth of single-layered α-Ni(OH) <sub>2</sub> nanosheets on a carbon cloth for highly efficient electrocatalytic oxidation of urea. Journal of Materials Chemistry A, 2018, 6, 13867-13873.	10.3	80
132	Adsorption separation of R134a, R125, and R143a fluorocarbon mixtures using 13X and surface modified 5A zeolites. AICHE Journal, 2018, 64, 640-648.	3.6	19
133	Unraveling Oxygen Evolution Reaction on Carbon-Based Electrocatalysts: Effect of Oxygen Doping on Adsorption of Oxygenated Intermediates. ACS Energy Letters, 2017, 2, 294-300.	17.4	145
134	Nickel–Cobalt Diselenide 3D Mesoporous Nanosheet Networks Supported on Ni Foam: An Allâ€pH Highly Efficient Integrated Electrocatalyst for Hydrogen Evolution. Advanced Materials, 2017, 29, 1606521.	21.0	370
135	Use of Platinum as the Counter Electrode to Study the Activity of Nonprecious Metal Catalysts for the Hydrogen Evolution Reaction. ACS Energy Letters, 2017, 2, 1070-1075.	17.4	366
136	Highly efficient and durable MoNiNC catalyst for hydrogen evolution reaction. Nano Energy, 2017, 37, 1-6.	16.0	79
137	Enhanced visible-light photocatalytic hydrogen production activity of three-dimensional mesoporous p-CuS/n-CdS nanocrystal assemblies. Inorganic Chemistry Frontiers, 2017, 4, 433-441.	6.0	47
138	Direct and selective hydrogenation of CO <sub>2</sub> to ethylene and propene by bifunctional catalysts. Catalysis Science and Technology, 2017, 7, 5602-5607.	4.1	118
139	In situ etching-induced self-assembly of metal cluster decorated one-dimensional semiconductors for solar-powered water splitting: unraveling cooperative synergy by photoelectrochemical investigations. Nanoscale, 2017, 9, 17118-17132.	5.6	88
140	Separation of Au Nanoplates and Nanoparticles through Density Gradient Centrifugation. Chemistry Letters, 2017, 46, 1570-1572.	1.3	1
141	Highly Concentrated, Ultrathin Nickel Hydroxide Nanosheet Ink for Wearable Energy Storage Devices. Advanced Materials, 2017, 29, 1703455.	21.0	62
142	Fabricating efficient CdSe–CdS photocatalyst systems by spatially resetting water splitting sites. Journal of Materials Chemistry A, 2017, 5, 20131-20135.	10.3	21
143	Unraveling the Intrinsic Structures that Influence the Transport of Charges in TiO <sub>2</sub> Electrodes. Advanced Energy Materials, 2017, 7, 1700886.	19.5	28
144	Effects of structure and size of Ni nanocatalysts on hydrogen selectivity via water-gas-shift reaction—A first-principles-based kinetic study. Catalysis Today, 2017, 280, 210-219.	4.4	24

#	Article	IF	CITATIONS
145	An ambipolar azaacene as a stable photocathode for metal-free light-driven water reduction. Materials Chemistry Frontiers, 2017, 1, 495-498.	5.9	33
146	Revisiting one-dimensional TiO2 based hybrid heterostructures for heterogeneous photocatalysis: a critical review. Materials Chemistry Frontiers, 2017, 1, 231-250.	5.9	67
147	Controllable synthesis of $\hat{l}$ ±-MoC1-x and $\hat{l}$ ²-Mo2C nanowires for highly selective CO2 reduction to CO. Catalysis Communications, 2016, 84, 147-150.	3.3	66
148	Full Characterization and Photoelectrochemical Behavior of Pyreneâ€fused Octaazadecacene and Tetraazaoctacene. Chemistry - an Asian Journal, 2016, 11, 482-485.	3.3	28
149	Nitrogen-doped cobalt phosphate@nanocarbon hybrids for efficient electrocatalytic oxygen reduction. Energy and Environmental Science, 2016, 9, 2563-2570.	30.8	216
150	Surface Rutilization of Anatase TiO <sub>2</sub> Nanorods for Creation of Synergistically Bridging and Fencing Electron Highways. Advanced Functional Materials, 2016, 26, 456-465.	14.9	52
151	Sustainable hydrogen and chemical production via photo-electrochemical reforming of biomass-derived alcohols. Nano Research, 2016, 9, 3388-3393.	10.4	20
152	Size Effects of Platinum Nanoparticles in the Photocatalytic Hydrogen Production Over 3D Mesoporous Networks of CdS and Pt Nanojunctions. Advanced Functional Materials, 2016, 26, 8062-8071.	14.9	98
153	Layer-by-layer assembly of nitrogen-doped graphene quantum dots monolayer decorated one-dimensional semiconductor nanoarchitectures for solar-driven water splitting. Journal of Materials Chemistry A, 2016, 4, 16383-16393.	10.3	59
154	A Molecular Relayâ€Modified CdSâ€5ensitized Photoelectrochemical Cell for Overall Water Splitting. ChemElectroChem, 2016, 3, 1471-1477.	3.4	4
155	Identification of Surface Reactivity Descriptor for Transition Metal Oxides in Oxygen Evolution Reaction. Journal of the American Chemical Society, 2016, 138, 9978-9985.	13.7	345
156	Tuning chemical bonding of MnO2 through transition-metal doping for enhanced CO oxidation. Journal of Catalysis, 2016, 341, 82-90.	6.2	132
157	Adsorption Separation of Râ€22, Râ€32 and Râ€125 Fluorocarbons using 4A Molecular Sieve Zeolite. ChemistrySelect, 2016, 1, 3718-3722.	1.5	20
158	Modulation of Crystal Surface and Lattice by Doping: Achieving Ultrafast Metal-Ion Insertion in Anatase TiO <sub>2</sub> . ACS Applied Materials & Interfaces, 2016, 8, 29186-29193.	8.0	23
159	Sulfur-Mediated Self-Templating Synthesis of Tapered C-PAN/g-C <sub>3</sub> N <sub>4</sub> Composite Nanotubes toward Efficient Photocatalytic H <sub>2</sub> Evolution. ACS Energy Letters, 2016, 1, 969-975.	17.4	86
160	In Situ Spectroscopic Identification of μ-OO Bridging on Spinel Co <sub>3</sub> O <sub>4</sub> Water Oxidation Electrocatalyst. Journal of Physical Chemistry Letters, 2016, 7, 4847-4853.	4.6	136
161	Identification of catalytic sites for oxygen reduction and oxygen evolution in N-doped graphene materials: Development of highly efficient metal-free bifunctional electrocatalyst. Science Advances, 2016, 2, e1501122.	10.3	1,078
162	Iridium Oxideâ€Assisted Plasmonâ€Induced Hot Carriers: Improvement on Kinetics and Thermodynamics of Hot Carriers. Advanced Energy Materials, 2016, 6, 1501339.	19.5	111

#	Article	IF	CITATIONS
163	Cadmium selenide-sensitized upright-standing mesoporous zinc oxide nanosheets for efficient photoelectrochemical H2 production. Journal of Energy Chemistry, 2016, 25, 371-374.	12.9	14
164	Niobium Doping Enhances Charge Transport in TiO <sub>2</sub> Nanorods. ChemNanoMat, 2016, 2, 660-664.	2.8	10
165	Linker-assisted assembly of 1D TiO2 nanobelts/3D CdS nanospheres hybrid heterostructure as efficient visible light photocatalyst. Applied Catalysis A: General, 2016, 521, 50-56.	4.3	23
166	Hierarchical carbon@Ni <sub>3</sub> S <sub>2</sub> @MoS <sub>2</sub> double core–shell nanorods for high-performance supercapacitors. Journal of Materials Chemistry A, 2016, 4, 1319-1325.	10.3	87
167	Achieving stable and efficient water oxidation by incorporating NiFe layered double hydroxide nanoparticles into aligned carbon nanotubes. Nanoscale Horizons, 2016, 1, 156-160.	8.0	99
168	Metal–Organic Frameworks as Promising Photosensitizers for Photoelectrochemical Water Splitting. Advanced Science, 2016, 3, 1500243.	11.2	100
169	Layer-by-layer assembly of versatile nanoarchitectures with diverse dimensionality: a new perspective for rational construction of multilayer assemblies. Chemical Society Reviews, 2016, 45, 3088-3121.	38.1	294
170	Tunneling Interlayer for Efficient Transport of Charges in Metal Oxide Electrodes. Journal of the American Chemical Society, 2016, 138, 3183-3189.	13.7	42
171	ZIF-8 derived carbon (C-ZIF) as a bifunctional electron acceptor and HER cocatalyst for g-C <sub>3</sub> N <sub>4</sub> : construction of a metal-free, all carbon-based photocatalytic system for efficient hydrogen evolution. Journal of Materials Chemistry A, 2016, 4, 3822-3827.	10.3	127
172	Graphdiyne: A Metal-Free Material as Hole Transfer Layer To Fabricate Quantum Dot-Sensitized Photocathodes for Hydrogen Production. Journal of the American Chemical Society, 2016, 138, 3954-3957.	13.7	335
173	In Operando Identification of Geometrical-Site-Dependent Water Oxidation Activity of Spinel Co <sub>3</sub> O <sub>4</sub> . Journal of the American Chemical Society, 2016, 138, 36-39.	13.7	787
174	1D TiO2 Nanotube-Based Photocatalysts. Green Chemistry and Sustainable Technology, 2016, , 151-173.	0.7	1
175	Doping-induced structural evolution from rutile to anatase: formation of Nb-doped anatase TiO <sub>2</sub> nanosheets with high photocatalytic activity. Journal of Materials Chemistry A, 2016, 4, 6926-6932.	10.3	36
176	Threading Chalcogenide Layers with Polymer Chains. Angewandte Chemie - International Edition, 2015, 54, 546-550.	13.8	102
177	One‣tep Hydrothermal Tailoring of NiCo <sub>2</sub> S <sub>4</sub> Nanostructures on Conducting Oxide Substrates as an Efficient Counter Electrode in Dye‣ensitized Solar Cells. Advanced Materials Interfaces, 2015, 2, 1500384.	3.7	83
178	Interim Anatase Coating Layer Stabilizes Rutile@Cr <sub><i>x</i></sub> O <sub><i>y</i></sub> Photoanode for Visibleâ€Lightâ€Driven Water Oxidation. ChemPhysChem, 2015, 16, 1352-1355.	2.1	8
179	Light-Induced In Situ Transformation of Metal Clusters to Metal Nanocrystals for Photocatalysis. ACS Applied Materials & Interfaces, 2015, 7, 28105-28109.	8.0	59
180	Oneâ€Dimensional Hybrid Nanostructures for Heterogeneous Photocatalysis and Photoelectrocatalysis. Small, 2015, 11, 2115-2131.	10.0	213

#	Article	IF	CITATIONS
181	Tin dioxide dodecahedral nanocrystals anchored on graphene sheets with enhanced electrochemical performance for lithium-ion batteries. Electrochimica Acta, 2015, 159, 46-51.	5.2	28
182	Parallel Near-Field Photolithography with Metal-Coated Elastomeric Masks. Langmuir, 2015, 31, 1210-1217.	3.5	21
183	Highly fluorescent polycaprolactones decorated with di(thiopheneâ€2â€yl)â€diketopyrrolopyrrole: A covalent strategy of tuning fluorescence properties in solid states. Journal of Polymer Science Part A, 2015, 53, 1032-1042.	2.3	18
184	Enhancement of photocatalytic properties of TiO2 nanoparticles doped with CeO2 and supported on SiO2 for phenol degradation. Applied Surface Science, 2015, 331, 17-26.	6.1	82
185	Ni <sup>3+</sup> â€Induced Formation of Active NiOOH on the Spinel Ni–Co Oxide Surface for Efficient Oxygen Evolution Reaction. Advanced Energy Materials, 2015, 5, 1500091.	19.5	408
186	Substrate-bound growth of Au–Pd diblock nanowire and hybrid nanorod–plate. Nanoscale, 2015, 7, 8115-8121.	5.6	12
187	Dye-sensitized polyoxometalate for visible-light-driven photoelectrochemical cells. Dalton Transactions, 2015, 44, 14354-14358.	3.3	43
188	A new surfactant-introduction strategy for separating the pure single-phase of metal–organic frameworks. Chemical Communications, 2015, 51, 9479-9482.	4.1	142
189	One-pot synthesis of ordered mesoporous Ni–V–Al catalysts for CO methanation. Journal of Catalysis, 2015, 326, 127-138.	6.2	127
190	Recent advances in methanation catalysts for the production of synthetic natural gas. RSC Advances, 2015, 5, 22759-22776.	3.6	411
191	A solution-processed, mercaptoacetic acid-engineered CdSe quantum dot photocathode for efficient hydrogen production under visible light irradiation. Energy and Environmental Science, 2015, 8, 1443-1449.	30.8	90
192	Fabrication and Photocatalytic Properties of TiO <sub>2</sub> /Reduced Graphene Oxide/Ag Nanocomposites with UV/Vis Response. European Journal of Inorganic Chemistry, 2015, 2015, 2222-2228.	2.0	24
193	Carbon nanotube catalysts: recent advances in synthesis, characterization and applications. Chemical Society Reviews, 2015, 44, 3295-3346.	38.1	586
194	ll–VI semiconductor nanowires. , 2015, , 3-28.		3
195	Bridging the Gap: Electron Relay and Plasmonic Sensitization of Metal Nanocrystals for Metal Clusters. Journal of the American Chemical Society, 2015, 137, 10735-10744.	13.7	141
196	Hierarchical Ni-Mo-S nanosheets on carbon fiber cloth: A flexible electrode for efficient hydrogen generation in neutral electrolyte. Science Advances, 2015, 1, e1500259.	10.3	427
197	N-Heteroheptacenequinone and N-heterononacenequinone: synthesis, physical properties, crystal structures and photoelectrochemical behaviors. Journal of Materials Chemistry C, 2015, 3, 9877-9884.	5.5	23
198	A flexible high-performance oxygen evolution electrode with three-dimensional NiCo2O4 core-shell nanowires. Nano Energy, 2015, 11, 333-340.	16.0	291

#	Article	lF	CITATIONS
199	Metallic Nanocatalysis: An Accelerating Seamless Integration with Nanotechnology. Small, 2015, 11, 268-289.	10.0	92
200	Assembly of a CdS quantum dot–TiO <sub>2</sub> nanobelt heterostructure for photocatalytic application: towards an efficient visible light photocatalyst via facile surface charge tuning. New Journal of Chemistry, 2015, 39, 279-286.	2.8	28
201	Metalâ€Clusterâ€Decorated TiO <sub>2</sub> Nanotube Arrays: A Composite Heterostructure toward Versatile Photocatalytic and Photoelectrochemical Applications. Small, 2015, 11, 554-567.	10.0	237
202	Biomolecule-assisted synthesis of carbon nitride and sulfur-doped carbon nitride heterojunction nanosheets: An efficient heterojunction photocatalyst for photoelectrochemical applications. Beilstein Journal of Nanotechnology, 2014, 5, 770-777.	2.8	15
203	Oneâ€Step Fabrication of Unique Mesoporous NiO Hollow Sphere Film on FTO for Highâ€Performance Pâ€Type Dyeâ€Sensitized Solar Cells. Advanced Materials Interfaces, 2014, 1, 1300110.	3.7	6
204	Hierarchical αâ€MnO <sub>2</sub> Nanowires@Ni <sub>1â€x</sub> Mn <sub>x</sub> O <sub>y</sub> Nanoflakes Core–Shell Nanostructures for Supercapacitors. Small, 2014, 10, 3181-3186.	10.0	118
205	Cadmium Sulfide Quantum Dots Supported on Gallium and Indium Oxide for Visibleâ€Lightâ€Driven Hydrogen Evolution from Water. ChemSusChem, 2014, 7, 2537-2544.	6.8	52
206	Formation of porous SnO2 microboxes via selective leaching for highly reversible lithium storage. Energy and Environmental Science, 2014, 7, 1013.	30.8	221
207	A p-type Ti( <scp>iv</scp> )-based metal–organic framework with visible-light photo-response. Chemical Communications, 2014, 50, 3786-3788.	4.1	424
208	Cesium Carbonate Functionalized Graphene Quantum Dots as Stable Electron-Selective Layer for Improvement of Inverted Polymer Solar Cells. ACS Applied Materials & Interfaces, 2014, 6, 1092-1099.	8.0	77
209	Layer-by-Layer Self-Assembly of CdS Quantum Dots/Graphene Nanosheets Hybrid Films for Photoelectrochemical and Photocatalytic Applications. Journal of the American Chemical Society, 2014, 136, 1559-1569.	13.7	413
210	A one-pot solvothermal synthesis of hierarchical microspheres with radially assembled single-crystalline TiO <sub>2</sub> -nanorods for high performance dye-sensitized solar cells. Journal of Materials Chemistry C, 2014, 2, 1381-1385.	5.5	25
211	All Inorganic Semiconductor Nanowire Mesh for Direct Solar Water Splitting. ACS Nano, 2014, 8, 11739-11744.	14.6	67
212	Self-assembly of aligned rutile@anatase TiO <sub>2</sub> nanorod@CdS quantum dots ternary core–shell heterostructure: cascade electron transfer by interfacial design. Materials Horizons, 2014, 1, 259-263.	12.2	69
213	Stable Quantum Dot Photoelectrolysis Cell for Unassisted Visible Light Solar Water Splitting. ACS Nano, 2014, 8, 10403-10413.	14.6	162
214	Recent advances in heterogeneous selective oxidation catalysis for sustainable chemistry. Chemical Society Reviews, 2014, 43, 3480.	38.1	653
215	{[M(NH3)6][Ag4M4Sn3Se13]}â^ž (M=Zn, Mn): Three-dimensional chalcogenide frameworks constructed from quaternary metal selenide clusters with two different transition metals. Journal of Solid State Chemistry, 2014, 218, 146-150.	2.9	20
216	Self-assembly of a Ag nanoparticle-modified and graphene-wrapped TiO <sub>2</sub> nanobelt ternary heterostructure: surface charge tuning toward efficient photocatalysis. Nanoscale, 2014, 6, 11293-11302.	5.6	64

#	Article	IF	CITATIONS
217	Doping high-surface-area mesoporous TiO <sub>2</sub> microspheres with carbonate for visible light hydrogen production. Energy and Environmental Science, 2014, 7, 2592.	30.8	253
218	High-surface-area mesoporous TiO <sub>2</sub> microspheres via one-step nanoparticle self-assembly for enhanced lithium-ion storage. Nanoscale, 2014, 6, 14926-14931.	5.6	25
219	Thermodynamically Driven One-Dimensional Evolution of Anatase TiO <sub>2</sub> Nanorods: One-Step Hydrothermal Synthesis for Emerging Intrinsic Superiority of Dimensionality. Journal of the American Chemical Society, 2014, 136, 15310-15318.	13.7	53
220	Electrochemical construction of hierarchically ordered CdSe-sensitized TiO <sub>2</sub> nanotube arrays: towards versatile photoelectrochemical water splitting and photoredox applications. Nanoscale, 2014, 6, 6727-6737.	5.6	85
221	Preparation and photoelectrochemical behavior of 1,4,6,8,11,13-hexazapentacene (HAP). Chemical Communications, 2014, 50, 7656-7658.	4.1	37
222	Spatially branched hierarchical ZnO nanorod-TiO <sub>2</sub> nanotube array heterostructures for versatile photocatalytic and photoelectrocatalytic applications: towards intimate integration of 1D–1D hybrid nanostructures. Nanoscale, 2014, 6, 14950-14961.	5.6	101
223	[enH][Cu <sub>2</sub> AgSnS <sub>4</sub> ]: a quaternary layered sulfide based on Cu–Ag–Sn–S composition. CrystEngComm, 2014, 16, 5989-5992.	2.6	40
224	One-dimensional metal oxide nanostructures for heterogeneous catalysis. Nanoscale, 2013, 5, 7175.	5.6	38
225	Large-Scale Synthesis of Transition-Metal-Doped TiO <sub>2</sub> Nanowires with Controllable Overpotential. Journal of the American Chemical Society, 2013, 135, 9995-9998.	13.7	326
226	Electrochemical fabrication of ZnO–CdSe core–shell nanorod arrays for efficient photoelectrochemical water splitting. Nanoscale, 2013, 5, 11118.	5.6	92
227	A general method for the synthesis of various rattle-type microspheres and their diverse applications. RSC Advances, 2013, 3, 18506.	3.6	12
228	Synergistic increase of oxygen reduction favourable Fe–N coordination structures in a ternary hybrid of carbon nanospheres/carbon nanotubes/graphene sheets. Physical Chemistry Chemical Physics, 2013, 15, 18482.	2.8	42
229	Self-assembly of hierarchically ordered CdS quantum dots–TiO2 nanotube array heterostructures as efficient visible light photocatalysts for photoredox applications. Journal of Materials Chemistry A, 2013, 1, 12229.	10.3	89
230	Anatase TiO2microspheres with reactive {001} facets for improved photocatalytic activity. RSC Advances, 2013, 3, 1222-1226.	3.6	32
231	A Fully Integrated Nanosystem of Semiconductor Nanowires for Direct Solar Water Splitting. Nano Letters, 2013, 13, 2989-2992.	9.1	506
232	Graphene quantum dots-incorporated cathode buffer for improvement of inverted polymer solar cells. Solar Energy Materials and Solar Cells, 2013, 117, 214-218.	6.2	64
233	Bioprobes Based on AIE Fluorogens. Accounts of Chemical Research, 2013, 46, 2441-2453.	15.6	1,607
234	Synthesis of single-crystalline anatase nanorods and nanoflakes on transparent conducting substrates. Chemical Communications, 2012, 48, 8565.	4.1	42

#	Article	IF	CITATIONS
235	Multilayer TiO2 nanorod cloth/nanorod array electrode for dye-sensitized solar cells and self-powered UV detectors. Nanoscale, 2012, 4, 3350.	5.6	66
236	One-dimensional copper hydroxide nitrate nanorods and nanobelts for radiochemical applications. Nanoscale, 2012, 4, 7194.	5.6	45
237	Photoelectrochemical Properties of TiO <sub>2</sub> Nanowire Arrays: A Study of the Dependence on Length and Atomic Layer Deposition Coating. ACS Nano, 2012, 6, 5060-5069.	14.6	378
238	High-Performance Plastic Dye-sensitized Solar Cells Based on Low-Cost Commercial P25 TiO <sub>2</sub> and Organic Dye. ACS Applied Materials & Interfaces, 2012, 4, 1709-1715.	8.0	47
239	Anatase TiO2 films with reactive {001} facets on transparent conductive substrate. Chemical Communications, 2011, 47, 9507.	4.1	66
240	Remarkable enhancement in photocurrent of In0.20Ga0.80N photoanode by using an electrochemical surface treatment. Applied Physics Letters, 2011, 99, .	3.3	27
241	Transferable and Flexible Nanorod-Assembled TiO <sub>2</sub> Cloths for Dye-Sensitized Solar Cells, Photodetectors, and Photocatalysts. ACS Nano, 2011, 5, 8412-8419.	14.6	209
242	TiO <sub>2</sub> –B/Anatase Core–Shell Heterojunction Nanowires for Photocatalysis. ACS Applied Materials & Interfaces, 2011, 3, 4444-4450.	8.0	162
243	Synthesis, formation mechanism and electric property of hollow InP nanospheres. Applied Physics A: Materials Science and Processing, 2011, 104, 61-68.	2.3	5
244	Layered mesoporous nanostructures for enhanced light harvesting in dye-sensitized solar cells. Journal of Renewable and Sustainable Energy, 2011, 3, 043106.	2.0	8
245	Oriented single-crystalline TiO <sub>2</sub> nanowires on titanium foil for lithium ion batteries. Journal of Materials Research, 2010, 25, 1588-1594.	2.6	34
246	Synthesis and Characterization of Singleâ€Crystalline Lanthanum Fluoride with a Ring‣ike Nanostructure. European Journal of Inorganic Chemistry, 2009, 2009, 2383-2387.	2.0	4
247	Direct growth of enclosed ZnO nanotubes. Nano Research, 2009, 2, 201-209.	10.4	71
248	Electron transport and recombination in dye-sensitized solar cells made from single-crystal rutile TiO2 nanowires. Physical Chemistry Chemical Physics, 2009, 11, 9648.	2.8	92
249	Growth of Oriented Single-Crystalline Rutile TiO <sub>2</sub> Nanorods on Transparent Conducting Substrates for Dye-Sensitized Solar Cells. Journal of the American Chemical Society, 2009, 131, 3985-3990.	13.7	2,243
250	Carbon Nanotubes Supported Mesoporous Mesocrystals of Anatase TiO2. Chemistry of Materials, 2008, 20, 2711-2718.	6.7	188
251	Oriented single crystalline titanium dioxide nanowires. Nanotechnology, 2008, 19, 505604.	2.6	138
252	Hollow ZnO Microspheres with Complex Nanobuilding Units. Chemistry of Materials, 2007, 19, 5824-5826.	6.7	98

#	Article	IF	CITATIONS
253	Optimization of High-Yield Biological Synthesis of Single-Crystalline Gold Nanoplates ChemInform, 2005, 36, no.	0.0	0
254	Symmetric and Asymmetric Ostwald Ripening in the Fabrication of Homogeneous Core-Shell Semiconductors. Small, 2005, 1, 566-571.	10.0	604
255	Ordered Alignment of CdS Nanocrystals on MWCNTs without Surface Modification. Journal of Physical Chemistry B, 2005, 109, 23783-23786.	2.6	55
256	Optimization of High-Yield Biological Synthesis of Single-Crystalline Gold Nanoplates. Journal of Physical Chemistry B, 2005, 109, 15256-15263.	2.6	197
257	Semiconductor Rings Fabricated by Self-Assembly of Nanocrystals. Journal of the American Chemical Society, 2005, 127, 18262-18268.	13.7	121
258	Salt-Assisted Deposition of SnO2 on α-MoO3 Nanorods and Fabrication of Polycrystalline SnO2 Nanotubes. Journal of Physical Chemistry B, 2004, 108, 5867-5874.	2.6	111
259	Room Temperature Solution Synthesis of Monodispersed Single-Crystalline ZnO Nanorods and Derived Hierarchical Nanostructures. Langmuir, 2004, 20, 4196-4204.	3.5	283
260	Fabrication of ZnO "Dandelions―via a Modified Kirkendall Process. Journal of the American Chemical Society, 2004, 126, 16744-16746.	13.7	539
261	Mesoscale Organization of CuO Nanoribbons:  Formation of "Dandelions― Journal of the American Chemical Society, 2004, 126, 8124-8125.	13.7	800
262	Hydrothermal Synthesis of ZnO Nanorods in the Diameter Regime of 50 nm. Journal of the American Chemical Society, 2003, 125, 4430-4431.	13.7	1,323